Received: 14 May 2022 | Revised: 20 July 2022 | Accepted: 21 July 2022

DOI: 10.1002/ptr.7586

LETTER TO THE EDITOR

WILEY

Phytoncides could potentially inhibit the spike protein of SARS-CoV-2 variants

Dear Editor-in-Chief

The spontaneous mutations are responsible for new severe acute respiratory syndrome coronavirus 2 (SARS-CoV-2) variants. World Health Organization designated delta B.1.617.2 and omicron B.1.1.529 variants as Variant of Concerns due to their high transmission, antibody neutralization, and mortality rate (WHO, 2021). The infection and mortality rate of the coronavirus disease-19 (COVID-19) condition are associated with a weaker immune system (Mohammadi, Shayestehpour, & Mirzaei, 2021). The phytoncides emitted from the plants exhibit antioxidant, anti-inflammatory, anti-microbial, and anti-viral properties (Roviello, Gilhen-Baker, Vicidomini, & Roviello, 2022; Thangaleela et al., 2022). Phytoncides improve the number and function of natural killer (NK) cells that significantly destruct the viral-infected cells and prevent the spreading of infection in the human body (Li, 2010).

Thus, in this study, we have screened the potential inhibitory efficacy of phytoncides against the S-protein of SARS-CoV-2 variants and compared it with the standard drug, cefuroxime. Totally one hundred and eighteen phytoncides were reported from the *Phyllostachys edulis*, *Liquidambar formosana*, and *Cunninghamia lanceolata* forests (Zhu et al., 2021), which were used against the receptor-binding domain (RBD) of Wuhan strain, delta B.1.617.2, and omicron B.1.1.529. The crystal structures of the Wuhan strain (PDB ID: 6LZG) (Wang et al., 2020), delta B.1.617.2 variant (PDB ID: 7E7B) (Ma et al., 2021), and omicron B.1.1.529 (PDB ID: 7T9L) (Mannar et al., 2022) were retrieved from protein data bank (Burley et al., 2017) for molecular docking analysis. Their interaction sites with the phytoncides are depicted in Figure S1. The target and phytoncides structures, optimization, molecular docking, and drug-likeness and toxicity analysis were performed as reported previously (Bharathi, Sivamaruthi, Kesika, Thangaleela, & Chaiyasut, 2022a; Bharathi, Sivamaruthi, Kesika, Thangaleela, & Chaiyasut, 2022b).

The molecular formula, weight, and PubChem ID were tabulated for the selected 85 phytoncides, which showed the potential interaction (binding affinity of ≤−5.0 kcal/mol) (Table S1). The phytoncides exhibited promising inhibitory effects against the studied SARS-CoV-2 variants. According to binding affinity and root-mean-square-deviation (RMSD) scores, neoabietic acid (−6.5 kcal/mol; RMSD = 2.2 Å) greatly bonded and potentially inhibited the residues of RBD of the Wuhan strain compared to cefuroxime (−5.9 kcal/mol; RMSD = 13.779 Å) (Figure 1a–c, Table 1). Likewise, octyl p-methoxycinnamate (−8.2 kcal/mol; RMSD = 1.895 Å) showed the possible inhibition against the RBD of delta B.1.617.2 variant compared to cefuroxime (−5.9 kcal/mol; RMSD = 2.323 Å) (Figure 1d–f, Table 1). Similarly, neoabietic acid (−6.4 kcal/mol; RMSD = 1.989 Å) manifested the potential inhibitory effect against the RBD of omicron B.1.1.529, while cefuroxime showed the binding affinity of −5.3 kcal/mol, and RMSD of 2.529 Å (Figure 1g–i, Table 1).

The neoabietic acid interacted with Wuhan and omicron B.1.1.529, octyl p-methoxycinnamate interacted with the delta B.1.617.2 variant with the maximum H-A and D-A distances of 2.70 and 3.35 Å, respectively (Figure 1j–l). Moreover, the docking results of other phytoncides that potentially inhibited RBD of Wuhan, delta B.1.617.2, and omicron B.1.1.529 variants are reported in Tables S2–-S4. Geranyllinalool, isophytol, squalene, and terpinolene significantly inhibited the crucial residues (LEU371 and PRO373) in the RBD of S-protein of omicron B.1.1.529, which were previously reported as the crucial mutations responsible for the immune escape mechanisms (CDC COVID-19 Response Team, 2021) (Table S4).

The toxicity analysis revealed that neoabietic acid and octyl p-methoxycinnamate comes under classes IV and VI, with possible lethal doses of 1,000 and 9,600 mg/kg of human body weight, respectively. Neoabietic acid and octyl p-methoxycinnamate are moderate carcinogenic and mutagenic, like the standard drug (cefuroxime), but they have a significant intestinal absorption rate compared to cefuroxime (Tables S5 and S6).

The results suggested that the phytoncides could effectively interact with the RBD domain of SARS-CoV-2 variants and may potentially inhibit the transmission of the virus. The results revealed that the natural volatile organic compounds, neoabietic acid, and octyl p-methoxycinnamate, emitted from the forest environment have a potent inhibitory effect against the RBD of SARs-CoV-2 variants than other tested phytoncides. Notably, geranyllinalool, isophytol, squalene, terpinolene, tributyl citrate, and 6,6-dimethylfulvene potentially inhibited the crucially mutated residues of omicron B.1.1.529.

The study results suggested that exposure to the natural forest environment (known as forest bathing) might provide immunity against SARs-CoV-2 infections. We hypothesized that the overall health improvement might be associated with the phytoncides' possible activation of the NK cells.

The results of this *in-silico* study were not confirmed in real-world situations. It is necessary to validate the inhibitory activities of the potent phytoncides against the interaction between angiotensin-converting enzyme 2 and RBD of S-protein of SARs-CoV-2 variants by binding or blocking experiments. Also, additional, in-depth studies are required to substantiate the findings that facilitate the development of phytoncides-based phytotherapeutic agents to treat COVID-19 infections.

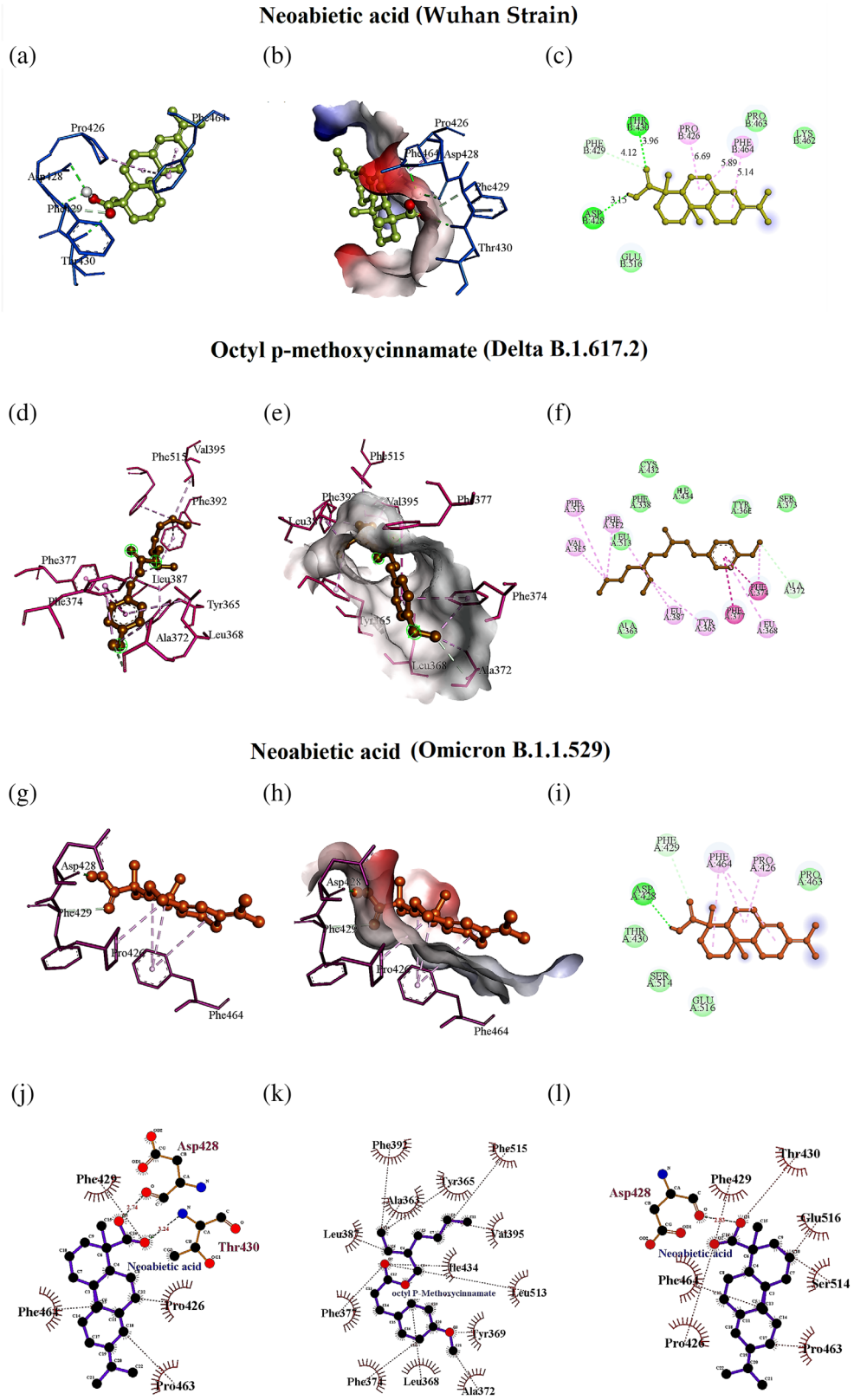

FIGURE 1 The interactions of representative phytoncides with S-protein of the Wuhan strain, delta B.1.617.2, and omicron B.1.1.529 (a, d, g). The ionizability surface of RBD residues with phytoncides was depicted (b, e, h) (Red indicates the ↑ acidic residues, blue indicates the ↑ basic residues). The type of bonds involved in the interaction of phytoncides and RBD residues of S-protein of SARs-CoV2 variants (c, f, i). The LigPlot^{+} schematics illustrate the interacted phytoncides and RBD (j–l).

TABLE 1 The binding affinity, RMSD, and interacting residues of the most effective phytoncides against the S-protein of RBD of the Wuhan strain (PDB ID: 6LZG), delta B.1.617.2 (PDB ID: 7E7B), and omicron B.1.1.529 (PDB ID: 7T9L)

SARs-CoV2-variants	Phytoncides	Binding affinity	RMSD (Å)	H/C-H bond interaction/pi	Interaction distances	Hydrophobic interaction	Alkyl/pi-alkyl interaction	Pi-sigma/cation stacked interaction
Wuhan strain	Cefuroxime	−5.9	13.779	ASN343, SER371, SER373[a], TRP436, ASN437, ASN440	5.82, 4.71, 4.05[a], 5.08, 5.72, 5.03	PHE342, VAL367, LEU368, SER438, LEU441, ARG509	—	—
	Neoabietic acid	−6.5	2.2	ASP428, PHE429[a], THR430	3.15, 4.12, 3.96	PRO426, LYS462, PRO463, GLU516	PHE464	—
	Octyl p-methoxycinnamate	−5.5	1.131	VAL362[a], ASP364	5.66, 3.93	CYS336, GLY339, PHE342, ASN343, VAL362, ALA363, LEU368, SER371, SER373	LEU335, PHE338, VAL367, PHE374	TRP436
Delta B.1.617.2	Cefuroxime	−5.9	2.323	ARG457, LYS458, ILE472, CYS480	3.83, 3.38, 4.12, 3.36	SER459, SER469, GLU471, TYR473, GLN474, GLY482	—	ASP467
	Octyl p-methoxycinnamate	−8.2	1.895	ALA372[a]	4.41	PHE338, ALA363, TYR365, TYR369, ALA372, SER373, VAL395, CYS432, ILE434, PHE515	LEU368, PHE374, LEU387, PHE392, LEU513	PHE374, PHE377
	Isophytol	−7.3	2.777	PHE374	3.45	PHE338, PHE342, LEU368, TYR369, ALA372, SER373	ALA363, TYR365, PHE374, PHE377, LEU387, VAL395, ILE434, LEU513, PHE515	TYR365, PHE392
	Neoabietic acid	−6.9	2.569	SER373	3.38	TYR365, LEU368, ALA372, PHE377	TYR369, PHE374	—
Omicron B.1.1.529	Cefuroxime	−5.3	2.529	THR376, LYS378, GLY404[a], ARG408, TYR508	4.49, 5.32, 5.15[a], 4.68, 5.67	PHE375, VAL407, ASN437	VAL503	—
	Neoabietic acid	−6.4	1.989	ASP428, PHE429[a]	4.15, 3.97	THR430, PRO463, SER514, GLU516	PRO426, PHE464	—
	Tributyl citrate	−5.0	1.344	ASP428[a], THR430, PHE515, GLU516[a]	4.53, 3.52, 6.15, 5.05	ARG355, TYR396, PHE429, PRO463, SER514	VAL382, PHE392, PRO426, PHE464, PHE515, LEU517	—

[a]Caron-hydrogen bond.

ACKNOWLEDGMENT

The authors gratefully acknowledge the Chiang Mai University, Chiang Mai, Thailand, for the support.

FUNDING INFORMATION

Chiang Mai University

CONFLICT OF INTEREST

The authors declare no conflicts of interest.

DATA AVAILABILITY STATEMENT

All the data have been provided in the manuscript and in supplementary materials.

Muruganantham Bharathi[1]
Bhagavathi Sundaram Sivamaruthi[2]
Periyanaina Kesika[1,2]
Subramanian Thangaleela[1]
Chaiyavat Chaiyasut[1]

[1]*Innovation Center for Holistic Health, Nutraceuticals, and Cosmeceuticals, Faculty of Pharmacy, Chiang Mai University, Chiang Mai, Thailand*
[2]*Office of Research Administration, Chiang Mai University, Chiang Mai, Thailand*

Correspondence
Bhagavathi Sundaram Sivamaruthi, Office of Research Administration, Chiang Mai University, Chiang Mai 50200, Thailand.
Email: sivamaruthi.b@cmu.ac.th

Chaiyavat Chaiyasut, Innovation Center for Holistic Health, Nutraceuticals, and Cosmeceuticals, Faculty of Pharmacy, Chiang Mai University, Chiang Mai 50200, Thailand.
Email: chaiyavat@gmail.com

ORCID

Muruganantham Bharathi https://orcid.org/0000-0003-3235-5837
Bhagavathi Sundaram Sivamaruthi https://orcid.org/0000-0002-5499-8350
Periyanaina Kesika https://orcid.org/0000-0002-3342-0947
Chaiyavat Chaiyasut https://orcid.org/0000-0002-1633-2419

REFERENCES

Bharathi, M., Sivamaruthi, B. S., Kesika, P., Thangaleela, S., & Chaiyasut, C. (2022a). *In silico* screening of potential phytocompounds from several herbs against SARS-CoV-2 Indian delta variant B.1.617.2 to inhibit the spike glycoprotein trimer. *Applied Sciences*, *12*(2), 665.

Bharathi, M., Sivamaruthi, B. S., Kesika, P., Thangaleela, S., & Chaiyasut, C. (2022b). *In silico* screening of bioactive compounds of representative seaweeds to inhibit SARS-CoV-2 ACE2-bound omicron B.1.1.529 spike protein trimer. *Marine Drugs*, *20*(2), 148.

Burley, S. K., Berman, H. M., Kleywegt, G. J., Markley, J. L., Nakamura, H., & Velankar, S. (2017). Protein data bank (PDB): The single global macromolecular structure archive. *Methods in Molecular Biology (Clifton, N.J.)*, *1607*, 627–641.

CDC COVID-19 Response Team. (2021). SARS-CoV-2 B.1.1.529 (Omicron) Variant - United States, December 1-8, 2021. *Morbidity and Mortality Weekly Report*, *70*(50), 1731-1734.

Li, Q. (2010). Effect of forest bathing trips on human immune function. *Environmental Health and Preventive Medicine*, *15*(1), 9–17.

Ma, J., Su, D., Sun, Y., Huang, X., Liang, Y., Fang, L., … Zheng, S. (2021). Cryo-EM structure of S-trimer, a subunit vaccine candidate for COVID-19. *Journal of Virology*, *95*(11), e00194–e00121.

Mannar, D., Saville, J. W., Zhu, X., Srivastava, S. S., Berezuk, A. M., Tuttle, K. S., … Subramaniam, S. (2022). SARS-CoV-2 omicron variant: Antibody evasion and cryo-EM structure of spike protein-ACE2 complex. *Science*, *375*(6582), 760–764.

Mohammadi, M., Shayestehpour, M., & Mirzaei, H. (2021). The impact of spike mutated variants of SARS-CoV2 [alpha, beta, gamma, delta, and lambda] on the efficacy of subunit recombinant vaccines. *The Brazilian Journal of Infectious Diseases*, *25*(4), 101606.

Roviello, V., Gilhen-Baker, M., Vicidomini, C., & Roviello, G. N. (2022). Forest-bathing and physical activity as weapons against COVID-19: A review. *Environmental Chemistry Letters*, *20*(1), 131–140.

Thangaleela, S., Sivamaruthi, B. S., Kesika, P., Bharathi, M., Kunaviktikul, W., Klunklin, A., … Chaiyasut, C. (2022). Essential oils, phytoncides, aromachology, and aromatherapy-a review. *Applied Sciences*, *12*(9), 4495.

Wang, Q., Zhang, Y., Wu, L., Niu, S., Song, C., Zhang, Z., … Qi, J. (2020). Structural and functional basis of SARS-CoV-2 entry by using human ACE2. *Cell*, *181*(4), 894–904.e9.

WHO. (2021). Classification of Omicron (B.1.1.529): SARS-CoV-2 Variant of Concern. Retrieved from https://www.who.int/news/item/26-11-2021-classification-of-omicron-[b.1.1.529]-sars-cov-2-variant-of-concern. Accessed March 10, 2022.

Zhu, S.-x., Hu, F.-f., He, S.-y., Qiu, Q., Su, Y., He, Q., & Li, J.-y. (2021). Comprehensive evaluation of healthcare benefits of different forest types: A case study in Shimen national forest park, China. *Forests*, *12*(2), 207.

SUPPORTING INFORMATION

Additional supporting information can be found online in the Supporting Information section at the end of this article.